BIOCHEMISTRY
including biophysical chemistry & molecular biology
Article

Biochemistry **2010,** *49,* 3545–3554 3545
DOI: 10.1021/bi100042b

The p12 Subunit of Human Polymerase δ Modulates the Rate and Fidelity of DNA Synthesis†

Xiao Meng, Yajing Zhou, Ernest Y. C. Lee, Marietta Y. W. T. Lee, and David N. Frick*

Department of Biochemistry and Molecular Biology, New York Medical College, Valhalla, New York 10595

Received January 12, 2010; Revised Manuscript Received March 19, 2010

ABSTRACT: This study examines the role of the p12 subunit in the function of the human DNA polymerase δ (Pol δ) holoenzyme by comparing the kinetics of DNA synthesis and degradation catalyzed by the four-subunit complex, the three-subunit complex lacking p12, and site-directed mutants of each lacking proofreading exonuclease activity. Results show that p12 modulates the rate and fidelity of DNA synthesis by Pol δ. All four complexes synthesize DNA in a rapid burst phase and a slower, more linear phase. In the presence of p12, the burst rates of DNA synthesis are ~5 times faster, while the affinity of the enzyme for its DNA and dNTP substrates appears unchanged. The p12 subunit alters Pol δ fidelity by modulating the proofreading 3′ to 5′ exonuclease activity. In the absence of p12, Pol δ is more likely to proofread DNA synthesis because it cleaves single-stranded DNA twice as fast and transfers mismatched DNA from the polymerase to the exonuclease sites 9 times faster. Pol δ also extends mismatched primers 3 times more slowly in the absence of p12. Taken together, the changes that p12 exerts on Pol δ are ones that can modulate its fidelity of DNA synthesis. The loss of p12, which occurs in cells upon exposure to DNA-damaging agents, converts Pol δ to a form that has an increased capacity for proofreading.

Each diploid cell in the human body contains more than 6 billion bp of DNA, which must be accurately copied before a cell can divide. The macromolecular machine that replicates human DNA must therefore function astonishingly fast, yet at the same time, this DNA "replisome" must be amazingly accurate (*1*). Thus, replicative DNA polymerases copy DNA with very low error rates. Extensive structural and kinetic studies have provided insights into how this fidelity is achieved. All DNA polymerases possess a common polymerase fold that resembles a right hand, which is formed by finger, palm, and thumb domains. The finger and thumb regions undergo conformational changes from an open to closed form upon binding of a dNTP,[1] providing for an extremely high level of selection for a correctly base paired incoming nucleotide as well as an appropriately base paired primer terminus (*2*−*6*). In addition, proofreading polymerases possess a 3′ to 5′ exonuclease domain (exo) that is distant from the polymerase site (pol), which further adds to the fidelity of DNA synthesis. The maintenance of genomic integrity also depends on a complex network of cellular responses to DNA damage that orchestrate cell cycle check points (*7*) and the repair of DNA damage (*8*).

Three DNA polymerases participate in eukaryotic chromosomal DNA replication. DNA polymerase δ (Pol δ) and ε are proofreading enzymes that possess pol and exo active sites, while polymerase α/primase synthesizes the primers on the lagging strand that are extended by the proofreading polymerases. Studies in budding yeast have provided evidence that Pol ε synthesizes most of the DNA on the leading strand template, while Pol δ synthesizes most of the DNA on the lagging strand template (*9*, *10*). However, the extent to which this division of labor takes place in the replication of the more complex genome of mammalian cells is still uncertain (*9*, *10*). Pol δ also plays a role in gap filling during DNA repair processes (*11*).

Human Pol δ has four subunits, p125, p50, p68, and p12 (*12*, *13*). The largest subunit, p125, is the catalytic subunit, and its catalytic domain is conserved with other members of the B family of DNA polymerases (*14*−*16*). The p125 subunit interacts with p50 to form the core enzyme; p68 interacts with p50, and p12 forms a bridge between p125 and p50 (*17*, *18*). The subunit composition of eukaryotic Pol δ is conserved between human and *Schizosaccharomyces pombe*, but the most extensively studied form of Pol δ, that of *Saccharomyces cerevisiae*, is a three-subunit enzyme, which lacks a homologue of p12 (*11*). The human Pol δ p125/p50/p68 trimer (Pol δ3) is active, in contrast to the less active p125/p50 dimer (*18*). The crystal structure of *S. cerevisiae* Pol δ (*19*) reveals extensive similarity between Pol δ and the monomeric bacteriophage RB69 polymerase, RB69 gp43, for which a number of structures have been obtained in different conformational states (*2*, *16*, *20*−*24*). RB69 gp43 shares homology with T4 polymerase, which has been more extensively studied (*25*).

Pol δ activity is involved in a number of DNA transactions that include not only DNA replication but also gap filling during DNA repair processes. Pol δ4 is converted into Pol δ3 by the depletion of the p12 subunit when cells are subjected to genotoxic stress by DNA-damaging agents such as ultraviolet light and methyl methanesulfonate, or by replication stress induced by treatment with hydroxyurea or aphidicolin (*26*). These findings

†This work was supported by grants from the National Institutes of Health (GM31973 and ES014737 to M.Y.W.T.L. and AI052395 to D.N.F.).

*To whom correspondence should be addressed. Phone: (914) 594-4190. Fax: (914) 594-5058. E-mail: David_Frick@nymc.edu.

[1]Abbreviations: dNTP, deoxynucleoside triphosphate; Exo, exonuclease active site; Pol, polymerase active site; Pol δ, human DNA polymerase δ; Pol δ3, Pol δ p125/p50/p68 trimer; Pol δ4, Pol δ p125/p50/p68/p12 tetramer.

Published on Web 03/25/2010

raise a number of questions about how the conversion of Pol δ4 to Pol δ3 might contribute to the DNA damage response. One way to gain insights into this question is to compare the properties of Pol δ3 with those of its progenitor. Comparison of the activities of Pol δ3 and Pol δ4 on damaged DNA templates reveals Pol δ3 is less able to bypass templates containing base lesions (O^6-MeG and 8-oxoG), produces more exonucleolytic products, and has a weakened tendency to insert wrong nucleotides and extend mismatched primers (*27*). Thus, Pol δ3 appears to display a classic "antimutator" phenotype (*28*), whereby an increase in exonucleolytic ability relative to the polymerase function enhances proofreading and fidelity.

In this study, we examined the kinetics of DNA synthesis and degradation catalyzed by Pol δ3 and Pol δ4 and their exonuclease-deficient mutants to provide insights into the nature of their functional differences. The rates of DNA synthesis were examined by pre-steady-state kinetic analysis and reveal that the loss of p12 decreases k_{pol}. Analysis of the rates of exonuclease activity reveals that the rate of translocation of DNA from pol to exo catalytic sites is increased when p12 is absent. Both changes are consistent with the exhibition of an antimutator phenotype for Pol δ3, in which Pol δ4 is less likely to proofread and more likely to extend mismatched primers. Thus, loss of p12 modulates both the rate and fidelity of DNA synthesis by facilitating a more rapid and frequent transfer of the DNA primer from the polymerase to the exonuclease active center. These findings provide novel insights into the role of p12 in human Pol δ function at the mechanistic level and into the potential cellular consequences of the in vivo conversion of Pol δ4 to Pol δ3.

EXPERIMENTAL PROCEDURES

Materials. Calf thymus DNA was obtained from Sigma-Aldrich (St. Louis, MO). dNTPs were obtained from GE Healthcare (Piscataway, NJ), and dGTP-α-thiotriphosphate (dGTP-αS) was obtained from Glen Research (Sterling, VA).

Recombinant human PCNA, recombinant unmodified Pol δ4, Pol δ3, and the D402A site-directed mutants of each (Pol $\delta4^{exo-}$ and Pol $\delta3^{exo-}$) were expressed in insect cells and purified as previously described (*27*, *29*). The Pol δ4 and Pol δ3 enzymes exhibited four and three major protein bands, respectively, on SDS−PAGE. Specific activities of the enzymes were similar to those previously reported (*27*). Pol δ enzyme concentrations for these studies were expressed as concentrations of the p125 subunit. This was determined by SDS−PAGE in which the purified Pol δ3 or Pol δ4 complexes were separated together with known amounts of catalase and aldolase (GE Healthcare) to generate standard curves after densitometry of the gels. Digital images of the stained gels were analyzed with AlphaEaseFC (Alpha Innotech, San Leandro, CA). Recombinant human PCNA was prepared as previously described (*29*). PCNA (400 nM) was included in all reaction mixtures. Such a concentration is at least 10 times more than is necessary to stimulate Pol δ to its maximal activity in any of the assays used in this study (Y. Zhou, X. Meng, and E. Y. C. Lee, unpublished data).

Polymerase Substrates. All DNA oligonucleotides were synthesized and PAGE-purified by Integrated DNA Technologies, Inc. (Coralville, IA). The sequences of the primers (25mer, 26merC, and 26merT) and the template (40mer) were as follows: 5′-GCC ACT ACA GCA CCT TGA CAG CCA G-3′ (25mer), 5′-GCC ACT ACA GCA CCT TGA CAG CCA G T-3′ (26merT), 5′-GCC ACT ACA GCA CCT TGA CAG CCA G C-3′ (26merC), and 5′-TCA TCG GTC GCA TCG CTG GCT GTC AAG GTG CTG TAG TGGC-3′ (40mer). The primers were 5′-labeled with ^{32}P using [γ-^{32}P]ATP (5000 Ci/mmol, MP Biochemicals) and T4 polynucleotide kinase (New England Biolabs). Labeled primers were purified using QIAquick Spin Columns (Qiagen), and concentrations were determined from the absorbance at 260 nm using extinction coefficients provided by Integrated DNA Technologies. Each primer was separately mixed with the template (40mer) in a ratio of 1:1.2 in 10 mM Tris-HCl (pH 7.5), incubated at 90 °C for 3 min, and gradually cooled to room temperature. All substrates were analyzed using nondenaturing PAGE to ensure that all primers were annealed.

Pre-Steady-State DNA Polymerase Assays. Reactions were conducted at 24 °C using a KinTek RQF-3 Rapid Quench Flow apparatus (KinTek Corp., Austin, TX). Pol δ preparations were first diluted in enzyme dilution buffer [8 μM PCNA, 50 mM bis(2-hydroxyethyl)iminotris(hydroxymethyl)methane (Bis-Tris) (pH 6.5), 5 mM dithiothreitol (DTT), 500 μg/mL bovine serum albumin (BSA), and 10% glycerol (v/v)], so that the concentrations of p125 and PCNA were 10 times the concentration to be loaded into syringe A. Syringe A contained 2× final concentrations of both Pol δ and DNA substrate, 800 nM PCNA (based on a trimeric molecular weight), 100 mM Bis-Tris (pH 6.5), 10 mM DTT, 400 μg/mL BSA, and 60 mM NaCl. After syringe A had been loaded, solutions were incubated at 24 °C for approximately 5 min. During this time, syringe B was loaded with 20 mM $MgCl_2$ and 2× final concentrations of dNTPs. Syringe C was loaded with 500 mM EDTA (pH 8).

We initiated reactions by rapidly mixing 20 μL from syringe A (Pol δ−PCNA−DNA complexes) with 20 μL from syringe B [$Mg(dNTP)^{2-}$ complexes] such that final reaction mixtures contained 50 mM Bis-Tris (pH 6.5), 5 mM DTT, 200 μg/mL BSA, 30 mM NaCl, 10 mM $MgCl_2$, 400 nM PCNA, dNTP, DNA, and Pol δ. After the indicated times, reactions were rapidly quenched by addition of 80 μL from syringe C (EDTA) such that the final concentration of EDTA was 330 mM. To analyze the remaining substrate and products, 20 μL of loading dye (95% formamide, 0.01% bromophenol blue, and 0.01% xylene cyanol) was added to 10 μL of each quenched reaction mixture. After these samples had been heated to 90 °C for 3 min, 4 μL of each was loaded on a 16% polyacrylamide (19:1 acrylamide:bisacrylamide)−8 M urea denaturing gel. After electrophoresis, [5′-^{32}P]DNA was visualized with a Molecular Dynamics Storm Phosphorimaging system and quantified with ImageQuant (Amersham Biosciences).

Transient-state time courses (products vs time) of polymerase reactions were fit to eq 1 to determine burst amplitude (ED), which is a measurement of the amount of the catalytically competent enzyme substrate present at the start of the reaction; the first-order rate constant describing the burst phase, k_{obs}; and the velocity of the linear phase of the reaction, *v*. GraphPad Prism version 4.0 (GraphPad, La Jolla, CA) was used for nonlinear regression.

$$[P] = [ED](1 - e^{-k_{obs}t}) + vt \quad (1)$$

To determine the K_d for the incoming dNTP and k_{pol}, we fit the k_{obs} values of reactions performed at various dNTP concentrations to eq 2.

$$k_{obs} = \frac{k_{pol}[dNTP]}{[dNTP] + K_{dNTP}} \quad (2)$$

Steady-state k_{cat} was calculated by eq 3.

$$v/E_t = \frac{k_{cat}[dNTP]}{[dNTP] + K_m} \quad (3)$$

where [dNTP] is the final dNTP concentration in the reaction, E_t is the amount of Pol δ determined by active site titration, v is the velocity from eq 1, and K_m is the Michaelis−Menten constant.

Single-Turnover Polymerase Assays. Single-turnover reactions for determining burst amplitudes were performed in the rapid quench apparatus using the same procedure as described above except that 1 mg/mL calf thymus DNA was also added to syringe B solutions so that the final concentration was 0.5 mg/mL. When 0.5 mg/mL calf thymus DNA was added to syringe A before mixing, no reaction was observed, confirming that this amount of enzyme trap is sufficient to force single-turnover conditions. In the presence of an enzyme trap, both Pol $\delta 4^{exo-}$ and Pol $\delta 3^{exo-}$ appear to catalyze only a single round of synthesis with the same amplitude as that observed in the burst phase of reactions without trap. We therefore determined amplitudes by simply stopping "single-turnover" reactions after the burst phase was complete. Typically, such reactions were stopped after 1 s, so that the amplitude of the single turnover could be measured.

To determine the equilibrium dissociation constant [K_{DNA} (Scheme 1)] describing binding of Pol δ and DNA, the products formed under single-turnover conditions, which reflect [ED], were fit to eq 4.

$$[ED] = \left[K_{DNA} + E_t + D_t - \sqrt{(K_{DNA} + E_t + D_t)^2 - 4E_tD_t}\right]/2 \quad (4)$$

where E_t is the total active site concentration, D_t is the total DNA concentration, and K_{DNA} is a dissociation constant describing the affinity of the enzyme for DNA.

Pre-Steady-State Exonuclease Assays. Exonuclease assays were performed in the rapid quench apparatus as described above for the polymerase assays except that no dNTPs (or calf thymus DNA) were included in syringe B, and 2× Pol δ solutions containing 100 nM p125 and each DNA substrate at 100 nM were added to syringe A. The final reaction mixtures contained 50 mM Bis-Tris (pH 6.5), 5 mM DTT, 200 μg/mL BSA, 30 mM NaCl, 10 mM $MgCl_2$, 400 nM PCNA, 50 nM DNA, and 100 nM Pol δ. Assays were performed with the 25mer primer as a single-stranded DNA substrate, with end-labeled 26merC/40mer as a double-stranded DNA and with 26merT/40mer as a substrate with a mispaired primer terminus.

Pseudo-first-order rate constants describing exonuclease reactions were determined by fitting time courses of the concentration of substrate remaining to eq 5.

$$[S] = [S_0]e^{-k_{obs}t} \quad (5)$$

where [S] is the concentration of substrate remaining at each time t, $[S]_0$ is the substrate concentration at the beginning of the reaction, and k_{obs} is a first-order rate constant describing either cleavage of DNA [k_{exo} (Scheme 1)] or transfer of DNA from the polymerase to exonuclease sites [$k_{pol\text{-}exo}$ (Scheme 1)].

Steady-State Polymerase/Exonuclease Assays. Assays monitoring the simultaneous action of the polymerase and exonuclease were performed at 37 °C. Pol δ (2 nM p125) was first incubated with 800 nM PCNA and 500 nM DNA substrate (25mer/40mer in the reaction in Figure 5A and 26merT/40mer in the reaction in Figure 5B) in 10 μL. Reactions were initiated by addition of 10 μL of a 2× final solution which has 20 mM $MgCl_2$ and 2 times the amounts of various dNTPs as indicated, such that final reaction mixtures contained 50 mM Bis-Tris (pH 6.5), 5 mM DTT, 200 μg/mL BSA, 30 mM NaCl, 10 mM $MgCl_2$, 400 nM PCNA, dNTP, 250 nM DNA, and Pol δ (2 μg/mL p125). After 3 min at 37 °C, reactions were stopped by removal of 6 μL and addition of it to 12 μL of loading buffer (25 mM EDTA in 95% formamide, 0.01% bromophenol blue, and 0.01% xylene cyanol). Reaction products were analyzed on gels as described above. Concentrations of products of the polymerase reaction ($[P_{pol}]$) and products of the exonuclease reaction ($[P_{exo}]$) were measured in each gel, and the percent of DNA edited was calculated using eq 6.

$$\text{edited } (\%) = \frac{[P_{exo}]}{[P_{exo}] + [P_{pol}]} \times 100 \quad (6)$$

RESULTS

The abilities of Pol δ4 and Pol δ3 to synthesize DNA have been compared previously only via examination of the ability of catalytic amounts of each complex to extend various primers annealed to various templates (*26*, *27*). In all these prior assays, Pol δ4 synthesized more DNA than Pol δ3, but it is not clear from those results whether Pol δ4 is a faster DNA polymerase than Pol δ3. It has long been established that the rate-limiting step in standard polymerase assays, where the enzyme is allowed to catalyze multiple reactions, is not DNA synthesis but rather template release (*30*, *31*). Similarly, prior assays indicating that Pol δ3 degrades DNA faster than Pol δ4 were conducted with limiting amounts of enzyme, so observed rates could reflect differences in the amounts of active enzyme in each preparation rather than different exonuclease functions per se (*27*). The goal of this study is to compare the polymerase and exonuclease functions of Pol δ4 and Pol δ3 under conditions where rates of DNA synthesis and degradation can be more accurately measured.

Human DNA Pol δ Synthesizes DNA Faster in the Presence of p12. To understand how p12 influences Pol δ-catalyzed DNA synthesis, we monitored reactions catalyzed by Pol δ4 and Pol δ3 in the presence of a 5′-end-labeled 25mer primer annealed to a 40mer template and a single complementary nucleotide, dCTP. Reactions were performed for very short incubation times (5 ms to 5 s) in a rapid quench apparatus, and 26mer products representing the addition of a single nucleotide were analyzed by polyacrylamide gel electrophoresis under denaturing conditions (Experimental Procedures). Both Pol δ4 and Pol δ3 synthesized DNA in a rapid burst phase followed by a slower, more linear phase that is characteristic of DNA polymerase-catalyzed DNA synthesis (Figure 1). The data were fit to a model typically used to analyze pre-steady-state DNA polymerase reactions (eq 1), in which the initial burst phase is described by a first-order rate constant and a linear velocity describes the second phase. For the experiment shown in Figure 1A, values for k_{obs} describing the fast phase of the reaction for Pol δ4 and Pol δ3 were 73 and 17 s^{-1}, respectively, showing that Pol δ4 was ~4 times faster than Pol δ3. The amplitudes of the burst phases were calculated to be 27 and 19 nM for Pol δ4- and Pol δ3-catalyzed reactions, respectively; these amplitudes likely reflect the concentrations of catalytically competent polymerase−substrate complexes present at the start of the reactions, which

Scheme 1: Reactions Involved in Pol δ-Catalyzed DNA Synthesis and Editing[a]

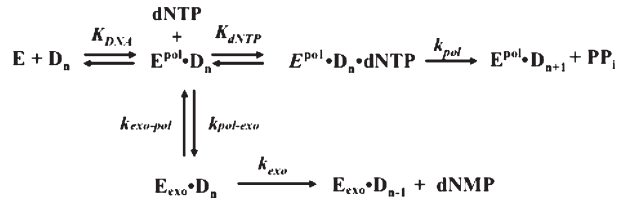

[a] E^{pol} and E_{exo} indicate DNA binding to pol sites and exo sites, respectively.

each contained 50 nM enzyme based on p125 protein content. Calculation of the rates of the linear portions of the reactions corrected for the concentration of active sites gave turnover numbers of 0.16 and 0.17 s^{-1} for Pol δ3 and Pol δ4, respectively.

In the gels that were used to analyze the experiments depicted in Figure 1A, we observed that small but significant amounts of exonucleolytic products were present in the reaction mixtures; these were more pronounced with Pol δ3 and were more prominent in the later linear phases of the reactions, so it is possible that the exonuclease activity of Pol δ3 may have caused reductions in the amount of product observed. Therefore, the same experiments were repeated using exonuclease-deficient forms of Pol δ. Pol $\delta4^{exo-}$ and Pol $\delta3^{exo-}$ each possess an alanine substitution for Asp402 in p125, a mutation that disrupts Pol δ exonuclease activity without affecting its polymerase function (*27*, *32*). The time courses of product formation for Pol $\delta4^{exo-}$ and Pol $\delta3^{exo-}$ are shown in Figure 1B. In this experiment, k_{obs} values of 54 and 13 s^{-1} were obtained for Pol $\delta4^{exo-}$ and Pol $\delta3^{exo-}$, respectively, a 4-fold difference. As with the wild-type enzymes, Pol $\delta4^{exo-}$ is 4 times faster than Pol $\delta3^{exo-}$. The rates of the linear (steady-state) phases divided by reaction amplitudes give turnover numbers for the reactions for Pol $\delta4^{exo-}$ and Pol $\delta3^{exo-}$ of 0.34 and 0.5 s^{-1}, respectively (Figure 1B). Thus, rates seen in the fast phase of the reaction were similar and rates in the slow phase slightly faster than when reactions were performed with wild-type Pol δ4 or Pol δ3, indicating that the exonuclease masks part of the polymerase activity in the native forms in the steady-state (slow) phase of the reactions.

Having shown that Pol δ4 extends a correctly base paired primer faster than Pol δ3, we next examined their abilities to extend a primer with a T:G mismatch at the primer terminus under the same conditions (Figure 1C). The rate constants for Pol $\delta4^{exo-}$ and Pol $\delta3^{exo-}$ were 7.6 and 2.5 s^{-1}, respectively (Figure 1C and Table 1). Both enzymes extended the mismatched primer more slowly than the matched primer, but Pol $\delta3^{exo-}$ was still 3 times slower than Pol $\delta4^{exo-}$.

The Apparent Affinities of Human Pol δ for DNA and dNTPs Are Not Influenced by p12. To probe whether the differences described above result from the possibility that p12 enhances the affinity of Pol δ for any of its substrates, we repeated the experiments described above at several different substrate concentrations. We used the exonuclease-deficient mutants of Pol δ4 and Pol δ3 for these experiments to prevent potential losses of product formation by exonuclease activity.

The affinities of Pol $\delta4^{exo-}$ and Pol $\delta3^{exo-}$ for DNA were estimated via examination of the kinetics of DNA synthesis at various DNA concentrations. The goal was to relate the amplitude of the burst phase of the reaction, which is commonly assumed to represent the number of catalytically competent enzyme−DNA complexes (active sites), to DNA concentration.

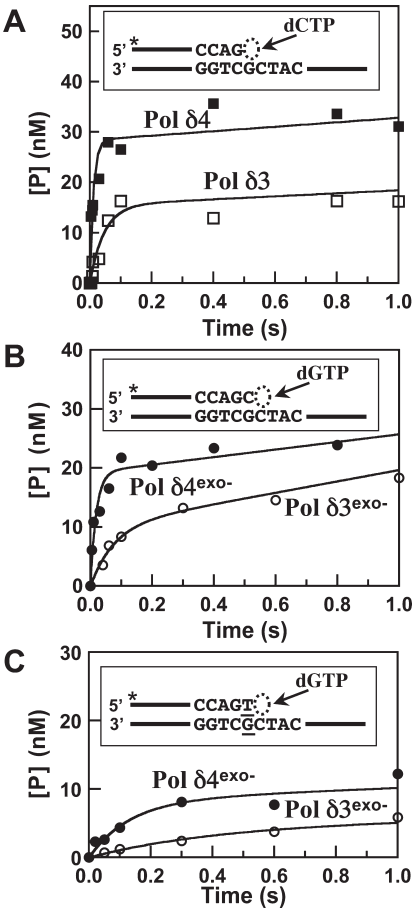

FIGURE 1: Pre-steady-state kinetics of DNA synthesis catalyzed by human Pol δ4 and Pol δ3. (A) Reactions with wild-type Pol δ4 and Pol δ3 were performed as described in Experimental Procedures using a rapid quench apparatus, and the reaction products representing addition of a single nucleotide to the primer were determined. Reaction mixtures contained Pol δ4 or Pol δ3 (50 nM p125), 500 nM [5′-^{32}P]25mer/40mer (see inset), and 500 μM dCTP. Primers extended by one nucleotide ([5′-^{32}P]26mer, [P]) are plotted vs time. Data are fit to eq 1 with the following parameters: (■) [ED] = 26.2 nM, k_{obs} = 72.7 s^{-1}, and v = 4.6 nM/s for Pol δ4; (□) [ED] = 18.6 nM, k_{obs} = 16.7 s^{-1}, and v = 3.0 nM/s for Pol δ3. (B) Pre-steady-state kinetics of DNA synthesis catalyzed by the exonuclease-deficient forms of Pol δ4 and Pol δ3. Reaction mixtures contained Pol $\delta4^{exo-}$ or Pol $\delta3^{exo-}$ (40 nM p125), 250 nM [5′-^{32}P]26merC/40mer (see inset), and 500 μM dGTP. Data are fit to eq 1 with the following constants: (●) [ED] = 19.3 nM, k_{obs} = 54.7 s^{-1}, and v = 6.4 nM/s for Pol $\delta4^{exo-}$; (○) [ED] = 10.0 nM, k_{obs} = 13.3 s^{-1}, and v = 9.6 nM/s for Pol $\delta3^{exo}$. (C) Pre-steady-state kinetics of DNA synthesis catalyzed by Pol $\delta4^{exo-}$ or Pol $\delta3^{exo-}$ in the presence of a mismatched DNA substrate: 40 nM p125, 200 nM mismatched [5′-^{32}P]26merT/40mer (see the inset; the T:G mismatch is underlined), and 500 μM dGTP. Data are fit to eq 1 using the following constants: k_{obs} = 7.6 s^{-1}, [ED] = 8.3 nM, and v = 1.9 nM/s for Pol $\delta4^{exo-}$; k_{obs} = 2.5 s^{-1}, [ED] = 4.4 nM, and v = 0.9 nM/s for Pol $\delta3^{exo-}$. Data for Pol δ4 and Pol δ3 are shown as filled and empty squares, respectively, and for Pol $\delta4^{exo-}$ and Pol $\delta3^{exo-}$ as filled and empty circles, respectively.

To first demonstrate that the fast phase of the reaction represents a single turnover, we repeated time courses in the presence of an enzyme trap (0.5 mg/mL calf thymus DNA) (Figure 2A). Addition of an enzyme trap did not significantly alter the burst amplitude, but it eliminated the slow phase of the reaction. Such results support the notion that the amplitude of the burst phase depends on the amount of enzyme−DNA complex present at the start of the reaction. To estimate the affinity of Pol δ^{exo-} for DNA, therefore, single-turnover reactions were performed in

Table 1: Estimates of Rate and Dissociation Constants Describing Pol δ-Catalyzed Reactions

	Pol δ4	Pol δ3	δ4/δ3[a]
k_{cat}[b]	0.24 ± 0.08 s^{-1}	0.18 ± 0.03 s^{-1}	1.3
k_{pol}[c]	87 ± 5.7 s^{-1}	19 ± 2.9 s^{-1}	4.6
K_{dNTP}[c]	3.6 ± 0.8 μM	3.2 ± 1.6 μM	1.0
K_{DNA}[d]	34 ± 5.4 nM	35 ± 6.5 nM	1.0
$k_{pol\ (mismatch)}$[e]	7.6 ± 2.4 s^{-1}	2.5 ± 0.6 s^{-1}	3.0
k_{exo}[f]	0.8 ± 0.2 s^{-1}	1.9 ± 0.4 s^{-1}	0.42
$k_{pol\text{-}exo}$[g]	0.003 ± 0.0004 s^{-1}	0.026 ± 0.003 s^{-1}	0.12
$k_{pol\text{-}exo\ (mismatch)}$[h]	0.062 ± 0.006 s^{-1}	0.29 ± 0.03 s^{-1}	0.21
$k_{pol\text{-}exo}$:k_{pol}[i]	1:29000	1:730	40
$k_{pol\text{-}exo\ (mismatch)}$:$k_{pol\ (mismatch)}$[i]	1:123	1:8.6	14

[a]Calculated by dividing the value observed with Pol δ4 by the value observed with Pol δ3. [b]Steady-state initial velocities of incorporation performed at various dNTP concentrations were fit to the Michaelis–Menten equation (eq 3) to determine a V_{max} (Figure 3H). The V_{max}/E_t relationship (active sites, Figure 3G) was use to determine a steady-state k_{cat}. Uncertainties are standard errors from three independent reaction sets. [c]Values were obtained by fitting eqs 1 and 2 to time courses obtained at various dNTP concentrations with Pol $\delta4^{exo-}$ or Pol $\delta3^{exo-}$ (Figure 3F). Errors are standard errors from nonlinear regression. [d]Values represent the average K_{DNA} obtained when eq 4 is used to fit three independent titrations with DNA (Figure 2B). Errors are standard deviations from three separate fits. [e]Observed first-order rate constant describing the burst phase for extension of a mismatched primer (Figure 1C). Errors are standard errors from nonlinear regression. [f]Observed first-order rate constant describing the degradation of single-stranded DNA (Figure 4A). Errors are standard errors from nonlinear regression. [g]Observed first-order rate constant describing the degradation of matched duplex DNA (Figure 4B). Errors are standard errors from nonlinear regression. [h]Observed first-order rate constants describing the degradation of mismatched duplex DNA (Figure 4C). Errors are standard errors from nonlinear regression. [i]The ratios indicate the probabilities for excision against extension of a primer terminus; alterations in the ratios when a mismatch terminus is present reflect the proofreading efficiency (*37*, *44*, *45*).

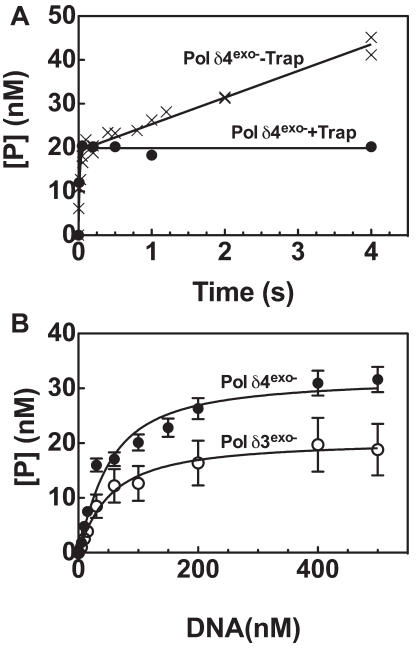

FIGURE 2: Effect of DNA primer/template concentration on the amplitude of the burst phase of DNA synthesis catalyzed by Pol $\delta4^{exo-}$ or Pol $\delta3^{exo-}$. (A) Effect of an enzyme trap. The reaction shown in Figure 1B (×) was repeated in the presence of an enzyme trap (0.5 mg/mL calf thymus DNA). The trap abolished the slow phase of the reaction catalyzed by Pol $\delta4^{exo-}$ (●), and data were fit to eq 1 with the following parameters: [ED] = 19.8 nM, k_{obs} = 94 s^{-1}, and v = 0 nM/s. (B) Single-turnover reaction mixtures (see Experimental Procedures) containing Pol $\delta4^{exo-}$ or Pol $\delta3^{exo-}$ (20 nM p125), 500 μM dGTP, 0.5 mg/mL calf thymus DNA, and the indicated amounts of [5′-^{32}P]26merC/40mer. The product concentration ([P]) at 1 s, which reflects the burst amplitude ([ED]) of the reaction, is plotted vs DNA concentration and fit to eq 3 with a K_{DNA} of 34 ± 5.4 nM for Pol $\delta4^{exo-}$ and a K_{DNA} of 35 ± 6.5 nM for Pol $\delta3^{exo-}$. Data for Pol $\delta4^{exo-}$ and Pol $\delta3^{exo-}$ are shown with filled and empty circles, respectively.

triplicate at various DNA concentrations (Figure 2B). The data were then fit to a one-site binding equation (eq 4), from which dissociation constants (K_{DNA}) of ~35 nM were found for both Pol $\delta4^{exo-}$ and Pol $\delta3^{exo-}$ (Table 1). Thus, p12 does not appear to affect the binding of DNA to Pol δ.

To examine how p12 affects the affinity of Pol δ for its dNTP substrates, burst assays were repeated with saturating levels of DNA (250 nM) in the presence of various dGTP concentrations for Pol $\delta4^{exo-}$ and Pol $\delta3^{exo-}$ as shown in Figure 3A–E. Under these conditions, the rates of the fast phase of the reaction (Figure 3F) and the rates of the slow phase (Figure 3H) increased with dGTP, as one would expect. Surprisingly, however, the amplitude of the fast phase of the reaction also increased (Figure 3G), implying that the concentration of catalytically competent complexes also varies with dGTP. Nevertheless, each factor describing the reactions increased similarly with dGTP regardless of whether Pol $\delta4^{exo-}$ or Pol $\delta3^{exo-}$ was present. We therefore chose to use the relationship between k_{obs} and dGTP concentration (Figure 3F) to estimate the maximum rate constant for DNA synthesis [k_{pol} (Scheme 1)] and the concentration of dGTP leading to half this rate (K_{dNTP}) by fitting the data to a one-binding site equation (eq 2), which is common practice (*33*).

The values of k_{pol} for Pol δ4 and Pol δ3 determined from these experiments were 87 ± 5.7 and 19 ± 2.9 s^{-1}, respectively. Values of K_{dNTP} for Pol $\delta4^{exo-}$ and Pol $\delta3^{exo-}$ for the incorporation of dGTP obtained in the same analysis for Pol $\delta4^{exo-}$ and Pol $\delta3^{exo-}$ were 3.6 ± 0.8 and 3.2 ± 1.6 μM, respectively, showing that binding affinities for dNTP are not affected by p12. Care should be exercised so as not to overinterpret these estimates since the reactions were clearly not performed under pseudo-first-order conditions despite the fact that best attempts were made to saturate the enzyme with all substrates besides dGTP. We also attempted to use these data to determine the Michaelis constants for Pol $\delta3^{exo-}$ and Pol $\delta4^{exo-}$, but because of errors in the rates of the slow phases, we were not able to determine an accurate K_m using the Michaelis–Menten equation for Pol $\delta4^{exo-}$. However, V_{max} values could be estimated to be 3.2 and 1.5 nM/s for Pol $\delta4^{exo-}$ and Pol $\delta3^{exo-}$, respectively. Adjusted for the maximal number of active sites determined in Figure 3G, k_{cat} values were estimated to be 0.24 and 0.18 s^{-1} for Pol $\delta4^{exo-}$ and Pol $\delta3^{exo-}$, respectively (Table 1).

p12 Modulates the Rate of Transfer of DNA between the Polymerase and Exonuclease Active Sites. We have previously examined the activities of Pol δ4 and Pol δ3 on oligonucleotide substrates and observed that Pol δ3 generated more exonucleolytic products, particularly when template lesions were encountered. Measurements of the exonuclease activities of Pol δ4 and Pol δ3 under steady-state conditions indicated that Pol δ3 might degrade DNA faster than Pol δ4 (*27*). However, to determine if p12 affects the true rates of the 3′ to 5′ exonuclease activity, we monitored rates of Pol δ4- and Pol δ3-catalyzed DNA cleavage in a rapid quench device under single-turnover conditions where the amount of enzyme exceeded the amount of DNA. The goal was to use pseudo-first-order reactions to estimate rate constants for DNA cleavage [k_{exo} (Scheme 1)]

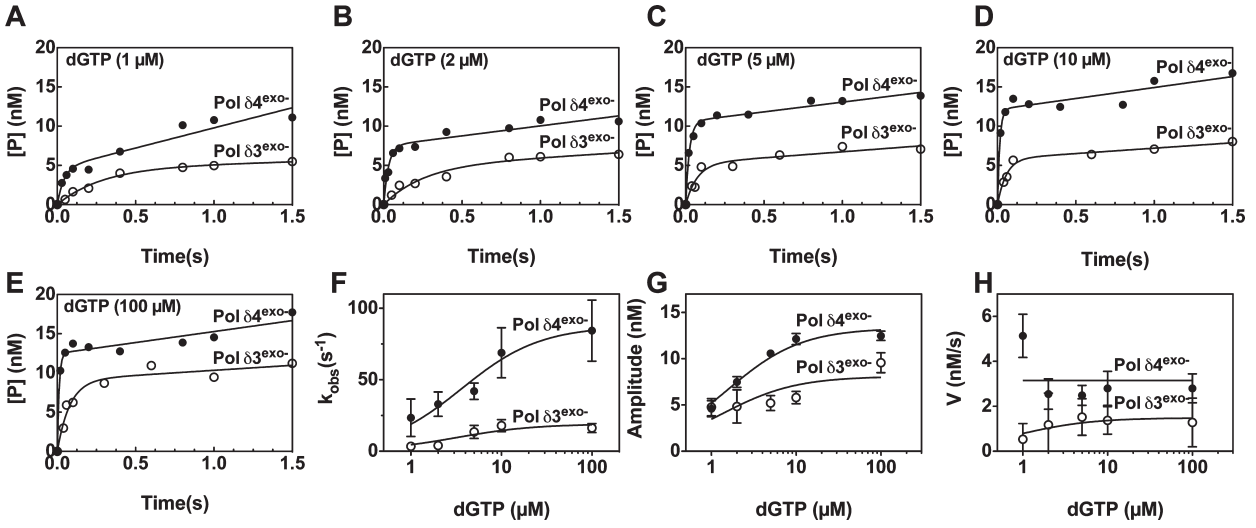

FIGURE 3: Effect of dNTP concentration on the pre-steady-state kinetics of Pol δ4- and Pol δ3-catalyzed DNA synthesis. Reaction mixtures contained Pol $\delta 4^{exo-}$ (●) or Pol $\delta 3^{exo-}$ (○), each at 20 nM p125, 250 nM [5′-^{32}P]26merC/40mer template (see the inset of Figure 1), and varying concentrations of dGTP [(A) 1, (B) 2, (C) 5, (D) 10, and (E) 100 μM]. Data were fit to eq 1. (F) k_{obs} values from fits in panels A−E as a function of dGTP concentration. Data are fit to eq 2 with a k_{pol} of 87 ± 12 s^{-1} and a K_d^{dGTP} of 3.6 ± 0.8 μM for Pol $\delta 4^{exo-}$ and a k_{pol} of 19 ± 2.8 s^{-1} and a K_{dGTP} of 3.2 ± 1.6 μM for Pol $\delta 3^{exo-}$. (G) Reaction amplitudes ([ED]) from the fits in panels A−E as a function of dGTP concentration. Data are fit to a one-binding site equation with a B_{max} of 13 ± 3 nM and a K_d of 1.6 ± 0.6 μM for Pol $\delta 4^{exo-}$ and a B_{max} of 8 ± 4 nM and a K_d of 1.3 ± 0.9 μM for Pol $\delta 3^{exo-}$. (H) Slow phase velocities (v) from fits in panels A−E as a function of dGTP concentration. Data are fit to eq 3 with a V_{max} of 3.1 ± 2.0 nM/s for Pol $\delta 4^{exo-}$ and a V_{max} of 1.4 ± 0.6 nM/s for Pol $\delta 3^{exo-}$ and a K_m of 0.8 ± 0.5 for Pol $\delta 3^{exo-}$. Data in panels A−F are from single reaction sets, but two additional assay sets were performed prior to the single reaction sets to determine appropriate time and concentration ranges. Fits to the other data sets yielded constants within the stated errors. Error bars and uncertainties reflect the standard error for the curve fits.

and for the transfer of the primer [$k_{pol\text{-}exo}$ (Scheme 1)] from the polymerase to the exonuclease site.

Kinetic studies (*34*) as well as structural studies have shown that during DNA synthesis, duplex DNA lies in the pol site while single-stranded DNA directly binds to the exo site (*2*, *20*, *21*). Three to four nucleotides of the primer must be melted so that the frayed primer can enter the exonuclease site, which typically can accommodate only ssDNA (*16*, *20*, *34*). Measurement of the rate of ssDNA hydrolysis, therefore, provides a determination of k_{exo}, the first-order rate constant describing the cleavage of a single nucleotide from the 3′ end of DNA (Scheme 1). Because duplex DNA binds to the pol site, k_{exo} measured with duplex DNA provides values for $k_{pol\text{-}exo}$, since switching of the primer to the exonuclease site is rate-limiting in such reactions (*3*).

Reaction mixtures containing Pol δ4 or Pol δ3 and a single-stranded oligonucleotide were quenched at various times (Figure 4A). The substrate remaining was fit to a first-order exponential decay equation (eq 5) to yield the rate constants (k_{exo}) describing hydrolytic cleavage. The value of k_{exo} obtained for Pol δ4 (0.8 s^{-1}) was approximately half that obtained for Pol δ3 (1.9 s^{-1}) (Figure 4A and Table 1). The values of k_{exo} for Pol δ have not been previously reported and are roughly 40-fold lower than values reported for RB69 polymerase (*23*).

Next, we determined the rate constants when similar reactions were performed with a 26mer/40mer duplex DNA (Figure 4B). This rate constant ($k_{pol\text{-}exo}$) for Pol δ3 was 0.026 s^{-1}, ∼9 times faster than that for Pol δ4 (0.003 s^{-1}) (Figure 4B and Table 1). When a 26mer/40mer with a T:G mismatch at the primer terminus was used, the switching rates for Pol δ4 and Pol δ3 were increased 20- and 10-fold, respectively, but the rate constant for Pol δ3 (0.29 s^{-1}) was still 5-fold faster than that for Pol δ4 (Figure 4C and Table 1).

These findings show that p12 exerts a large negative effect on the rate at which the primer terminus is switched from the polymerase to the exonuclease site and only a small effect (∼2-fold) on k_{exo}. Thus, Pol δ3 would be expected to exhibit an enhanced proofreading ability compared to that with Pol δ4. Along with the negative effect on k_{pol} when p12 is absent, it is apparent that these two effects both lead to an increased proofreading capacity for Pol δ3. Changes in k_{pol} or $k_{pol\text{-}exo}$ have been shown to alter the proofreading or fidelity of DNA polymerases and to generate mutator or antimutator phenotypes (*3*, *35*−*37*). To understand the combined effects of alterations in $k_{pol\text{-}exo}$ and k_{pol}, it is useful to examine the $k_{pol\text{-}exo}$:k_{pol} ratio, as an indication of the probability of excision of the primer terminus, and thus the proofreading activity. The ratio is 1:29000 for Pol δ4 and 1:730 for Pol δ3 on an unmodified template (Table 1). This ∼40-fold difference indicates that Pol δ3 is more active in proofreading than Pol δ4. When assayed on a template with a mismatched primer terminus, the ratios for Pol δ4 and Pol δ3 were 1:123 and 1:8.6, respectively (Table 1). The increase in the ratio of either enzyme when compared to that of the normal template reflects the increased probabilities for the excision of the mismatch. Comparison of the ratios for the mismatched primer terminus shows that Pol δ3 is 14 times more likely to remove a mismatched primer terminus than Pol δ4.

Taken together, our findings show that removal of p12 leads to reciprocal changes in k_{pol} and the switching rate, $k_{pol\text{-}exo}$, that are known to result in an increased level of proofreading, which is associated with a capacity for increased fidelity of DNA synthesis.

In the Absence of p12, Human Pol δ Is More Likely To Proofread Errors. The data given above clearly show that in the presence of p12, human Pol δ synthesizes DNA more rapidly and degrades DNA more slowly. Slower DNA cleavage in the presence of p12 seems to arise not from an intrinsically slower exonuclease but rather from a slower transfer of the DNA from the polymerase to the exonuclease site. To examine how these

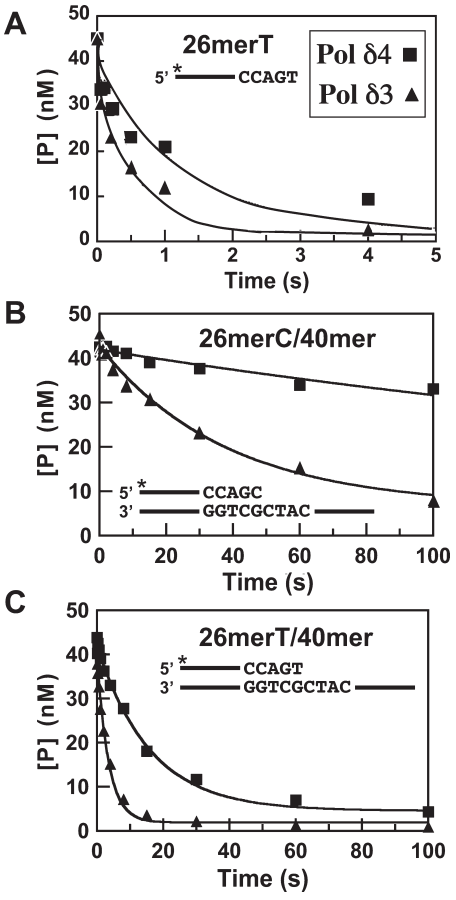

FIGURE 4: Determination of the rates of exonuclease cleavage of ssDNA and dsDNA by Pol δ4 and Pol δ3. Reactions were performed as described in Experimental Procedures using a rapid quench apparatus under single-turnover conditions. The final reaction mixtures contained Pol δ3 or Pol δ4 (100 nM p125) and 50 nM DNA substrate. Reactions were initiated by addition of 10 mM Mg^{2+} and quenched at various times (from 0.05 to 150 s). The remaining 26mer was determined, and the data were fit into an exponential decay equation (eq 5) and yield observed rates of excision. (A) Time course of hydrolysis of a 26mer ssDNA, [5′-^{32}P]26merT, by Pol δ4 (■) and Pol δ3 (▲). Values for the rates are given as k_{exo} in Table 1. (B) Time course of hydrolysis of a 26mer/40mer duplex DNA, [5′-^{32}P]26merC/40mer, by Pol δ4 (■) and Pol δ3 (▲). Values for the rates are given in Table 1 as the rates for switching of the primer terminus from the pol to the exo site [$k_{pol\text{-}exo}$ (Scheme 1)]. (C) Time course of hydrolysis of a 26mer/40mer duplex DNA containing a mismatched primer terminus, [5′-^{32}P]26merT/40mer, by Pol δ4 (■) and Pol δ3 (▲). Values for the rates are given in Table 1 as the rates for switching of the primer terminus from the pol to the exo site [$k_{pol\text{-}exo\ (mismatch)}$].

differences might impact the fidelity of DNA synthesis, we examined Pol δ action under conditions that might force the enzyme to introduce a mutation. Pol δ4 and Pol δ3 were incubated with the 25mer/40mer in the presence of concentrations of the next correct nucleotide, dCTP, ranging from 5 μM to 10 mM or the dNTPs that do not base pair with the template. Products formed under steady-state conditions were examined to determine the percentage of DNA that was edited, which was defined as the amount of exonucleolytic products as a percentage of the sum of exonucleolytic (< 26mer) and extension products (> 26mer) (eq 6, Experimental Procedures). In the presence of dCTP, editing is suppressed with increasing dCTP concentrations since the insertion of dCTP suppresses the appearance of exonucleolytic products; when it is plotted against log[dNTP], a linear relationship is observed. It is apparent that Pol δ3 is far more active than Pol δ4 in editing (Figure 5). When the incorrectly base paired dNTPs are present, very high concentrations are required to suppress editing; nevertheless, it is Pol δ3 that again exhibits greater editing activity than Pol δ4. We performed a similar analysis in an experiment with a substrate in which the primer contained a T:G mismatch, and only the next correct nucleotide, dGTP, was added in increasing concentrations. Once the terminal mismatch is removed, the dGTP represents a mismatched dNTP, and thus editing activity prevails. This is seen for Pol δ3, for which inhibition of editing dominates and essentially no primer extension can be observed until ~1 mM dGTP. Pol δ4 exhibited a lower extent of editing initially, and this could be suppressed at much lower dGTP concentrations than with Pol δ3. While the conditions used are forcing, in that they require high concentrations of dNTPs, these experiments provide a demonstration that Pol δ3 exhibits a greater degree of fidelity than Pol δ4, since this editing assay monitors in tandem their different propensities for insertion of a wrong nucleotide and for excision of a mismatched primer terminus.

DISCUSSION

We have investigated the kinetic properties of human Pol δ4 and Pol δ3 with two goals in mind, to understand the role of the p12 subunit in Pol δ catalysis and to gain insights into a rationale for the removal of the p12 subunit during DNA damage, based on their altered properties. We examined the polymerase and exonuclease functions of Pol δ4 and Pol δ3 using pre-steady-state kinetic methods to obtain values for kinetic parameters that might provide more information about how p12 alters the catalytic functions of Pol δ. Pre-steady-state kinetic analyses have provided powerful tools for understanding the kinetic mechanisms of DNA polymerase functions and have complemented the structural studies that have led to current models for the mechanisms whereby the exquisite fidelity of DNA polymerases is achieved (*3*, *4*).

The experiments described above have provided estimates of the constants in Scheme 1: K_{DNA}, K_{dNTP}, k_{pol}, $k_{pol\text{-}exo}$, and k_{exo} for Pol δ4 and Pol δ3 (Table 1). Note that Scheme 1 is simpler than minimal kinetic mechanisms that have been determined for other DNA polymerases like those encoded by bacteriophage or prokaryotes (*25*, *38*) in that the various steps in DNA synthesis are not delineated. In other words, k_{pol} in Scheme 1 may include more than one substep, such as a conformational change and chemical step. Scheme 1 is also intended to mainly highlight the fact that because the exonuclease active site (exo) is spatially separated from the polymerase active site (pol) (*6*), the primer terminus has to be translocated, or switched, to the exo site for proofreading to take place (*3*, *34*). Kinetic analyses of polymerase mutants have provided significant insights into understanding how alterations in the rates of these parameters affect the fidelity of DNA polymerases. Alterations in the switching rates from pol to exo sites ($k_{pol\text{-}exo}$) affect the efficiency of proofreading, while reductions in k_{pol} that occur by mutation or by encounter of a mismatched terminus lead to a kinetic barrier that favors translocation of the DNA from the pol to the exo site (*3*, *35*). Our findings show that two key rate constants, k_{pol} and $k_{pol\text{-}exo}$, are affected by the absence or presence of p12 in the Pol δ enzyme.

The difference in k_{pol} implies that p12 accelerates the rate of DNA synthesis by ~4.6-fold. The k_{pol} of 87 s^{-1} for Pol δ4 is higher than the value of 21 s^{-1} previously reported for the p125/p50 dimer calf thymus Pol δ (*39*), which is closer to the k_{pol} of 19 s^{-1} for Pol δ3 (Table 1). However, since the calf thymus

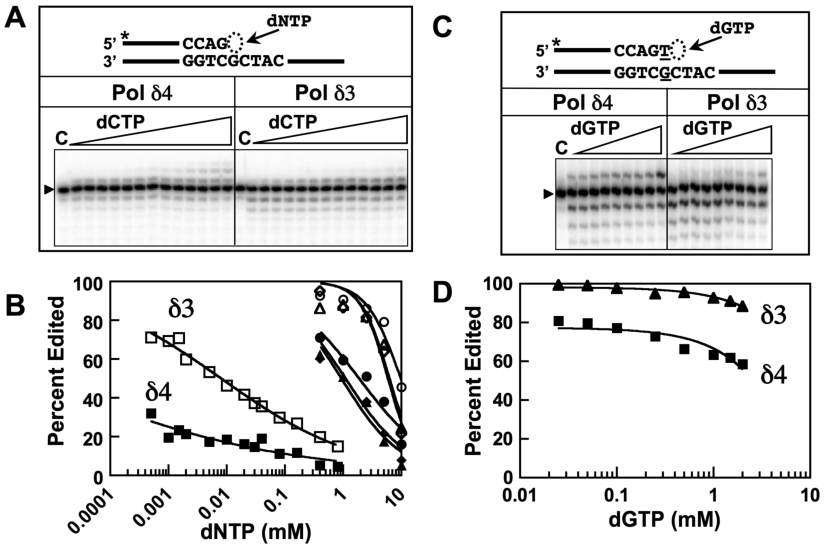

FIGURE 5: Steady-state rates of Pol δ polymerase and exonuclease activities in the presence of varying concentrations of the correct or incorrect nucleotide. Reaction mixtures contained catalytic amounts (2 nM p125) of wild-type Pol δ4 or Pol δ3, the indicated templates at 250 nM, and individual dNTPs as indicated (Experimental Procedures). (A) Product formation by Pol δ4 or Pol δ3 on a matched primer (25mer/40mer, inset). The gel shows the product formation when the reactions were performed with increasing concentrations of the correct nucleotide, dCTP (0.5, 1, 1.5, 2, 5, 10, 20, 30, 40, 80, 160, 400, and 800 mM). Lane C is a control with no enzyme added, and the arrowhead indicates the position of the 25mer primer. (B) Reactions with dCTP or the individual incorrect nucleotides were performed as described for panel A. Percentages of substrate that were edited by Pol δ were calculated as the percentages of the total exonucleolytic products over the sum of the exonucleolytic and extension products (eq 6) and plotted as percent edited vs log[dNTP]: (squares) dCTP, (triangles) dATP, (circles) dTTP, and (diamonds) dGTP. Data for Pol δ4 are shown as filled symbols and those for Pol δ3 as empty symbols. (C) Product formation by Pol δ4 or Pol δ3 on a mismatched primer (26merT/40mer, inset). Reactions were performed as described for panel A, and the products formed with dGTP, the next correct nucleotide, are shown in the gel. dGTP concentrations of 0.025, 0.05, 0.10, 0.25, 0.5, 1.0, 1.5, and 2.0 mM were used. Lane C is a control with no enzyme added, and the arrowhead indicates the position of the 26merT primer. (D) Percentages of substrate that were edited by Pol δ4 (■) and Pol δ3 (▲) were calculated as described for panel B and plotted vs log[dGTP]. No extension was observed with either Pol δ4 or Pol δ3 in the presence of dATP, dTTP, or dGTP.

experiments were performed at a higher temperature (37 °C) than our studies (24 °C), such a comparison might not be meaningful. Nevertheless, these findings show that p12 has a crucial role in modulating Pol δ catalysis, in which it is able to modulate the rate-limiting step(s) involved in the catalysis of phosphodiester bond formation. This capacity has important implications for the changes that take place when p12 is removed; decreases in k_{pol} have been shown to form a kinetic barrier that increases the probability of switching of the primer terminus from the pol to the exo site, thereby providing a basis for enhanced proofreading (*3*). Thus, p12 acts as a gearshift that regulates k_{pol} in a manner that will alter the proofreading capacity of Pol δ.

The second step altered by p12 is $k_{pol\text{-}exo}$, a rate constant describing the switching of the primer terminus from the pol to the exo sites, a step that plays a critical role in proofreading. This alteration has significant implications for the effects of p12 on the capacity of Pol δ to perform proofreading. The alterations of the balance between polymerase and exonuclease activities that we observed are ones that are shown to alter the proofreading of DNA polymerases and to generate mutator or antimutator phenotypes in related enzymes that reduce the mutation frequency during replication (*3*, *35*−*37*). We have performed experiments that assess the degree of editing by Pol δ4 and Pol δ3 on oligonucleotide substrates and observed the expected increase in the level of editing (Figure 5). The characteristics displayed by Pol δ3 allow us to predict that it would display greater fidelity when synthesizing DNA in vitro, and possibly in vivo. Future studies will be needed to obtain quantitative assessments of alterations in the fidelity of DNA synthesis by Pol δ4 and Pol δ3.

Our findings are illustrated in the diagram in Figure 6A, which shows the directional shifts in k_{pol}, $k_{pol\text{-}exo}$, and the $k_{pol\text{-}exo}/k_{pol}$ ratio when p12 is absent or present. The function of p12 can be viewed as that of a gearshift. The presence of p12 increases the rate of polymerization and slows the switching rate. When p12 is removed from the Pol δ complex, there is a downshift in the rate of phosphodiester bond formation. This will facilitate proofreading via the kinetic barrier effect, in which reduction of k_{pol} favors the probability of translocation of the primer terminus from the pol to exo sites. Coupled with this, removal of p12 increases the rates of translocation of primer from the pol to exo site, a change that further enhances proofreading. Thus, p12 functions as a gearshift whose effect on the catalytic properties of Pol δ changes two of the key rate constants that govern proofreading efficiency. Taken together, our data provide a mechanistic basis for the earlier observations that Pol δ3 exhibits behaviors consistent with an increased level of proofreading (*27*).

The structural basis for the influence of p12 on both pol and exo functions is unknown, and at this point, one can only speculate about how p12 might exert its effects on Pol δ. Comparison of structures of RB69 polymerase with yeast Pol δ (*19*) can provide some insights into the mechanisms by which a primer terminus is switched from the pol to the exo sites (*2*, *16*, *20*−*24*, *40*). These studies have shown that there are large DNA movements as well as protein conformational changes that take place upon switching between the editing and polymerization modes (Figure 6B). In particular, movement of the tip of the thumb domain (*21*) and a β-hairpin loop (*23*, *40*) must occur for DNA to migrate from the pol to the exo site for editing to take place. Notably, in contrast to analogous RB69 structures, the recent yeast Pol δ structure (*19*) reveals this

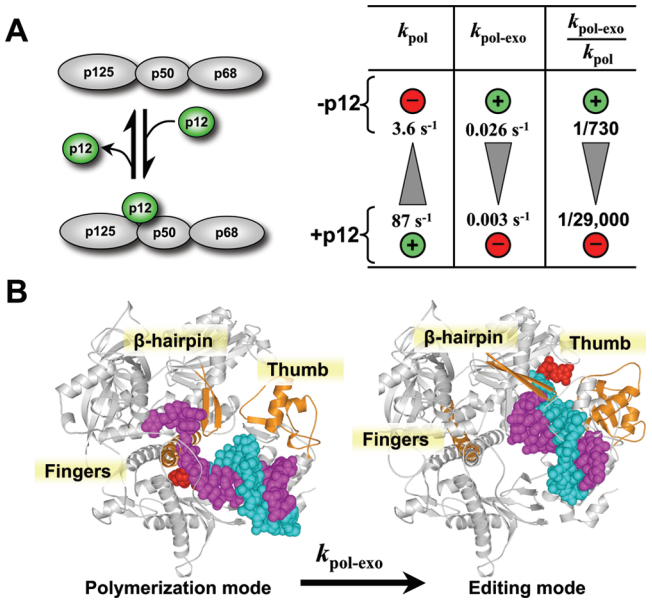

FIGURE 6: p12 subunit of Pol δ that acts as a gearshift that alters the rates of polymerization and primer switching. (A) Diagram of the effects of p12 on Pol δ. The first two columns show the effects of p12 on the kinetic constants for polymerization (k_{pol}) and translocation of the primer terminus from the pol to the exo site ($k_{pol\text{-}exo}$), respectively. The third column shows the effects on proofreading efficiency, expressed as the $k_{pol\text{-}exo}$:k_{pol} ratio. The shaded triangles indicate the direction of change of the rate constants from low to high, and the circled plus and minus signs indicate the effects of the presence and absence of p12, respectively, on the rate constants. (B) Models of the switch of the DNA from the pol to the exo sites of Pol δ. The model on the left is the recently published structure of the yeast Pol δ catalytic subunit (*19*) in the polymerization mode, viz., in a ternary complex bound to a primer (cyan), template (magenta), and nucleoside triphosphate (red) [Protein Data Bank (PDB) entry 1IAY]. The model on the right shows a putative structure of yeast Pol δ in the editing mode, which was made by aligning the yeast Pol δ structure (PDB entry 1IAY) and a structure of the related RB69 polymerase (PDB entry 1CLQ) with DNA bound in the exonuclease site (*20*). The RB69 and Pol δ structures superimpose except along one helix in the finger domain, the tip of the thumb domain, and a β-hairpin. These three regions of RB69 are shown (orange) to point out the conformational changes needed to transfer the primer between the pol and exo sites. The finger, thumb, and β-hairpin structures of yeast Pol δ are highlighted (orange) in the model on the left. The rest of the RB69 protein is not shown for the sake of clarity, but the primer (cyan), the primer 3′ terminus (red), and template (magenta) bound to RB69 are shown to mark the exonuclease site of Pol δ (gray).

β-hairpin (β16−β17) in a conformation where it directly interacts with the template strand, consistent with an involvement with primer switching between pol and exo sites. Thumb movement, however, might be even more critical as evidenced by the fact that some of the first antimutator alleles discovered map to this region of the related T4 DNA polymerase (*41*), and the mutations have now been shown to clearly affect primer switching in the T4 enzyme (*37*, *42*). Effects of p12 on the reduction of the rate of switching of the primer from the pol to the exo site ($k_{pol\text{-}exo}$) could be exerted by an interaction with such regions of Pol δ. p12 could exert effects on conformational changes, cause steric interference of the movement of the primer terminus, or modify access to the exonuclease site (*23*, *43*). Alternatively, p12 might impede primer movement in a channel crossed by the primer terminus during shuttling of the primer between pol and exo sites (*44*).

Our findings also provide insight into how loss of p12 might alter the biological function of the human replisome. Agents that damage DNA cause p12 to rapidly disappear in cells (*26*), and the results described above show that this change causes Pol δ to shift to a form that has enhanced proofreading ability and has previously been shown to exhibit reduced capacity for lesion bypass synthesis (*27*). More proofreading would be needed when the genome is damaged, especially if such damage leads to base modifications that cause nucleotides to base pair ambiguously. As previously discussed, loss of the p12 subunit could affect a number of the DNA transactions in which Pol δ is engaged in vivo, e.g., its ability to interact with other proteins involved in DNA damage or its ability to participate in DNA repair processes (*26*). This study provides significant new mechanistic information that may assist in evaluating the role of Pol δ3 in cells that have undergone DNA damage.

NOTE ADDED AFTER ASAP PUBLICATION:

The version of this paper that was published online April 2, 2010 was missing several minor text changes. The corrected version was reposted April 7, 2010.

REFERENCES

1. Nachman, M. W., and Crowell, S. L. (2000) Estimate of the mutation rate per nucleotide in humans. *Genetics 156*, 297–304.
2. Steitz, T. A. (1999) DNA polymerases: Structural diversity and common mechanisms. *J. Biol. Chem. 274*, 17395–17398.
3. Johnson, K. A. (1993) Conformational coupling in DNA polymerase fidelity. *Annu. Rev. Biochem. 62*, 685–713.
4. Kunkel, T. A., and Bebenek, K. (2000) DNA replication fidelity. *Annu. Rev. Biochem. 69*, 497–529.
5. Doublie, S., Sawaya, M. R., and Ellenberger, T. (1999) An open and closed case for all polymerases. *Structure 7*, R31–R35.
6. Steitz, T. A., and Yin, Y. W. (2004) Accuracy, lesion bypass, strand displacement and translocation by DNA polymerases. *Philos. Trans. R. Soc. London, Ser. B 359*, 17–23.
7. Branzei, D., and Foiani, M. (2007) Interplay of replication checkpoints and repair proteins at stalled replication forks. *DNA Repair 6*, 994–1003.
8. Harper, J. W., and Elledge, S. J. (2007) The DNA damage response: Ten years after. *Mol. Cell 28*, 739–745.
9. Kunkel, T. A., and Burgers, P. M. (2008) Dividing the workload at a eukaryotic replication fork. *Trends Cell Biol. 18*, 521–527.
10. Burgers, P. M. (2009) Polymerase dynamics at the eukaryotic DNA replication fork. *J. Biol. Chem. 284*, 4041–4045.
11. Garg, P., and Burgers, P. M. (2005) DNA polymerases that propagate the eukaryotic DNA replication fork. *Crit. Rev. Biochem. Mol. Biol. 40*, 115–128.
12. Liu, L., Mo, J., Rodriguez-Belmonte, E. M., and Lee, M. Y. (2000) Identification of a fourth subunit of mammalian DNA polymerase δ. *J. Biol. Chem. 275*, 18739–18744.
13. Mo, J., Liu, L., Leon, A., Mazloum, N., and Lee, M. Y. (2000) Evidence that DNA polymerase δ isolated by immunoaffinity chromatography exhibits high-molecular weight characteristics and is associated with the KIAA0039 protein and RPA. *Biochemistry 39*, 7245–7254.
14. Yang, C. L., Chang, L. S., Zhang, P., Hao, H., Zhu, L., Toomey, N. L., and Lee, M. Y. (1992) Molecular cloning of the cDNA for the catalytic subunit of human DNA polymerase δ. *Nucleic Acids Res. 20*, 735–745.
15. Hao, H., Jiang, Y., Zhang, S. J., Zhang, P., Zeng, R. X., and Lee, M. Y. (1992) Structural and functional relationships of human DNA polymerases. *Chromosoma 102*, S121–S127.
16. Wang, J., Sattar, A. K., Wang, C. C., Karam, J. D., Konigsberg, W. H., and Steitz, T. A. (1997) Crystal structure of a pol α family replication DNA polymerase from bacteriophage RB69. *Cell 89*, 1087–1099.
17. Xie, B., Mazloum, N., Liu, L., Rahmeh, A., Li, H., and Lee, M. Y. (2002) Reconstitution and characterization of the human DNA polymerase δ four-subunit holoenzyme. *Biochemistry 41*, 13133–13142.
18. Li, H., Xie, B., Zhou, Y., Rahmeh, A., Trusa, S., Zhang, S., Gao, Y., Lee, E. Y., and Lee, M. Y. (2006) Functional roles of p12, the fourth subunit of human DNA polymerase δ. *J. Biol. Chem. 281*, 14748–14755.

19. Swan, M. K., Johnson, R. E., Prakash, L., Prakash, S., and Aggarwal, A. K. (2009) Structural basis of high-fidelity DNA synthesis by yeast DNA polymerase δ. *Nat. Struct. Mol. Biol. 16*, 979–986.
20. Shamoo, Y., and Steitz, T. A. (1999) Building a replisome from interacting pieces: Sliding clamp complexed to a peptide from DNA polymerase and a polymerase editing complex. *Cell 99*, 155–166.
21. Franklin, M. C., Wang, J., and Steitz, T. A. (2001) Structure of the replicating complex of a pol α family DNA polymerase. *Cell 105*, 657–667.
22. Hogg, M., Wallace, S. S., and Doublie, S. (2004) Crystallographic snapshots of a replicative DNA polymerase encountering an abasic site. *EMBO J. 23*, 1483–1493.
23. Hogg, M., Aller, P., Konigsberg, W., Wallace, S. S., and Doublie, S. (2007) Structural and biochemical investigation of the role in proofreading of a β hairpin loop found in the exonuclease domain of a replicative DNA polymerase of the B family. *J. Biol. Chem. 282*, 1432–1444.
24. Aller, P., Rould, M. A., Hogg, M., Wallace, S. S., and Doublie, S. (2007) A structural rationale for stalling of a replicative DNA polymerase at the most common oxidative thymine lesion, thymine glycol. *Proc. Natl. Acad. Sci. U.S.A. 104*, 814–818.
25. Karam, J. D., and Konigsberg, W. H. (2000) DNA polymerase of the T4-related bacteriophages. *Prog. Nucleic Acid Res. Mol. Biol. 64*, 65–96.
26. Zhang, S., Zhou, Y., Trusa, S., Meng, X., Lee, E. Y., and Lee, M. Y. (2007) A novel DNA damage response: Rapid degradation of the p12 subunit of DNA polymerase δ. *J. Biol. Chem. 282*, 15330–15340.
27. Meng, X., Zhou, Y., Zhang, S., Lee, E. Y., Frick, D. N., and Lee, M. Y. (2009) DNA damage alters DNA polymerase δ to a form that exhibits increased discrimination against modified template bases and mismatched primers. *Nucleic Acids Res. 37*, 647–657.
28. Muzyczka, N., Poland, R. L., and Bessman, M. J. (1972) Studies on the biochemical basis of spontaneous mutation. I. A comparison of the deoxyribonucleic acid polymerases of mutator, antimutator, and wild type strains of bacteriophage T4. *J. Biol. Chem. 247*, 7116–7122.
29. Zhang, P., Zhang, S. J., Zhang, Z., Woessner, J. F. J., and Lee, M. Y. (1995) Expression and physicochemical characterization of human proliferating cell nuclear antigen. *Biochemistry 34*, 10703–10712.
30. Bryant, H. E., Schultz, N., Thomas, H. D., Parker, K. M., Flower, D., Lopez, E., Kyle, S., Meuth, M., Curtin, N. J., and Helleday, T. (2005) Specific killing of BRCA2-deficient tumours with inhibitors of poly(ADP-ribose) polymerase. *Nature 434*, 913–917.
31. Byrnes, J. J., Downey, K. M., Que, B. G., Lee, M. Y., Black, V. L., and So, A. G. (1977) Selective inhibition of the 3′ to 5′ exonuclease activity associated with DNA polymerases: A mechanism of mutagenesis. *Biochemistry 16*, 3740–3746.
32. Goldsby, R. E., Hays, L. E., Chen, X., Olmsted, E. A., Slayton, W. B., Spangrude, G. J., and Preston, B. D. (2002) High incidence of epithelial cancers in mice deficient for DNA polymerase δ proofreading. *Proc. Natl. Acad. Sci. U.S.A. 99*, 15560–15565.
33. Johnson, K. A. (1995) Rapid quench kinetic analysis of polymerases, adenosinetriphosphatases, and enzyme intermediates. *Methods Enzymol. 249*, 38–61.
34. Donlin, M. J., Patel, S. S., and Johnson, K. A. (1991) Kinetic partitioning between the exonuclease and polymerase sites in DNA error correction. *Biochemistry 30*, 538–546.
35. Khare, V., and Eckert, K. A. (2002) The proofreading 3′→5′ exonuclease activity of DNA polymerases: A kinetic barrier to translesion DNA synthesis. *Mutat. Res. 510*, 45–54.
36. Reha-Krantz, L. J. (1995) Learning about DNA polymerase function by studying antimutator DNA polymerases. *Trends Biochem. Sci. 20*, 136–140.
37. Reha-Krantz, L. J. (1998) Regulation of DNA polymerase exonucleolytic proofreading activity: Studies of bacteriophage T4 "antimutator" DNA polymerases. *Genetics 148*, 1551–1557.
38. Capson, T. L., Peliska, J. A., Kaboord, B. F., Frey, M. W., Lively, C., Dahlberg, M., and Benkovic, S. J. (1992) Kinetic characterization of the polymerase and exonuclease activities of the gene 43 protein of bacteriophage T4. *Biochemistry 31*, 10984–10994.
39. Einolf, H. J., and Guengerich, F. P. (2000) Kinetic analysis of nucleotide incorporation by mammalian DNA polymerase δ. *J. Biol. Chem. 275*, 16316–16322.
40. Subuddhi, U., Hogg, M., and Reha-Krantz, L. J. (2008) Use of 2-aminopurine fluorescence to study the role of the β hairpin in the proofreading pathway catalyzed by the phage T4 and RB69 DNA polymerases. *Biochemistry 47*, 6130–6137.
41. Reha-Krantz, L. J. (1989) Locations of amino acid substitutions in bacteriophage T4 tsL56 DNA polymerase predict an N-terminal exonuclease domain. *J. Virol. 63*, 4762–4766.
42. Stocki, S. A., Nonay, R. L., and Reha-Krantz, L. J. (1995) Dynamics of bacteriophage T4 DNA polymerase function: Identification of amino acid residues that affect switching between polymerase and 3′ → 5′ exonuclease activities. *J. Mol. Biol. 254*, 15–28.
43. Hadjimarcou, M. I., Kokoska, R. J., Petes, T. D., and Reha-Krantz, L. J. (2001) Identification of a mutant DNA polymerase δ in *Saccharomyces cerevisiae* with an antimutator phenotype for frameshift mutations. *Genetics 158*, 177–186.
44. Wu, P., Nossal, N., and Benkovic, S. J. (1998) Kinetic characterization of a bacteriophage T4 antimutator DNA polymerase. *Biochemistry 37*, 14748–14755.
45. Nick McElhinny, S. A., Stith, C. M., Burgers, P. M., and Kunkel, T. A. (2007) Inefficient proofreading and biased error rates during inaccurate DNA synthesis by a mutant derivative of *Saccharomyces cerevisiae* DNA polymerase δ. *J. Biol. Chem. 282*, 2324–2332.